

Edge states in Graphene: from gapped flat band to gapless chiral modes

Wang Yao,^{1,2} Shengyuan A. Yang,¹ and Qian Niu¹

¹*Department of Physics, The University of Texas, Austin, TX 78712-0264*

²*Department of Physics, and Center of Theoretical and Computational Physics, The University of Hong Kong, Hong Kong*
(Dated: October 14, 2008)

We study edge-states in graphene systems where a bulk energy gap is opened by inversion symmetry breaking. We find that the edge-bands dispersion can be controlled by potentials applied on the boundary with unit cell length scale. Under certain boundary potentials, gapless edge-states with valley-dependent velocity are found, exactly analogous to the spin-dependent gapless chiral edge-states in quantum spin Hall systems. The connection of the edge-states to bulk topological properties is revealed.

PACS numbers: 73.20.-r, 73.63.-b, 81.05.Uw

One of the most intriguing phenomena in solid state physics is the existence of edge-state on the boundary of a 2D system. The edge-state can have distinct properties from the bulk band and play important roles in transport. When the system has a band structure in which empty bands and fully occupied bands are separated by an energy gap, current can not flow in the bulk. However, this does not dictate the system to be a simple insulator, as conduction may still be allowed by edge-states on the boundary. Well known examples are the quantum Hall effect (QHE) and the quantum spin Hall effect (QSHE), where gapless chiral edge-states are robust channels with quantized conductance [1, 2, 3, 4, 5, 6]. On the other hand, the property of the edge-states are intimately related to the property of the bulk band. For example, in QHE and QSHE, the existence and chiral nature of gapless edge-states are found to be the consequence of bulk topological orders [7, 8, 9, 10, 11, 12].

The recent realization of graphene in laboratories has attracted extensive interests to this 2D lattice [13, 14, 15]. Its bulk band structure has two degenerate and inequivalent valleys centered at the corners of the first Brillouin zone (known as the Dirac points). The free standing graphene crystallite is a zerogap semiconductor where the conduction and valance band touch each other at the Dirac points. A bulk energy gap can be opened by breaking the inversion symmetry, e.g. by a staggered sublattice potential in single layer graphene, or by an interlayer bias in graphene bilayer. The neutral graphene system then becomes a normal insulator, with vanishing Hall conductance and spin Hall conductance. Nevertheless, it does acquire a nontrivial bulk topological property: the two inequivalent valleys each carry a non-zero topological charge with opposite signs, giving rise to the valley-dependent Hall effect [16, 17]. Not by coincidence, edge-states also exist in such graphene systems with peculiar behaviors [18, 19, 20, 21, 22, 23, 24]. For graphene sheet terminated with zigzag edges, edge-states form a one dimensional band which connects the two Dirac points with completely flat dispersion. Because of its unusual dispersion relation, the edge-bands in graphene have been exploited for a number of interesting phenomena including valley-filtered transport [25], magnetism [26, 27, 28, 29], and superconductivity [30].

In this work, we study edge-state behaviors in graphene systems with broken bulk inversion symmetry. We find that

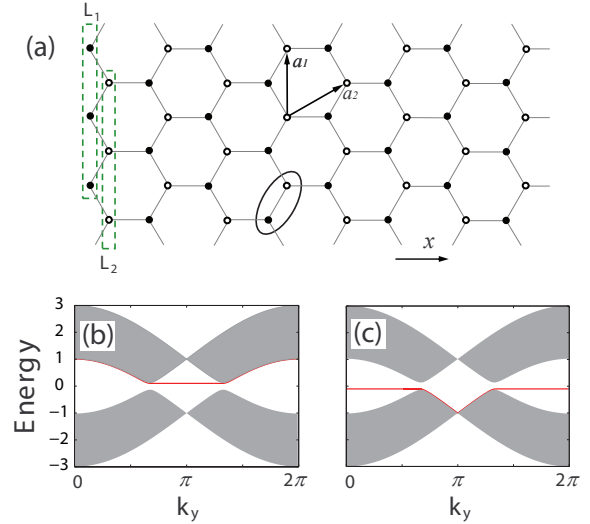


FIG. 1: (Color online) (a) Schematic illustration of a single layer graphene with zigzag edge on the left boundary. The two triangular sublattices are denoted by ● and ○ respectively. A unit cell contains one atom from each sublattice (denoted by the oval). (b) Band structure of graphene with a zigzag edge. (c) Band structure of graphene with a bearded edge (i.e. with column L_2 removed in (a)). In (b) and (c), only the edge-states on the left boundary are shown (red curves). A staggered sublattice potential $\Delta/2 = 0.1$ is universally applied in the bulk and on the boundary (see text).

the edge-band dispersion can be continuously changed by simply tuning the on-site energies on the boundary of the system. Under certain values of the boundary potential, the edge-band can either completely merge into the bulk band structure, or become valley-dependent gapless chiral modes. In the latter case, for single layer graphene (bilayer graphene), each boundary of the system carries two (four) gapless edge-states, one (two) at each valley, with opposite velocities. Therefore, when the Fermi energy lies in the bulk gap, we have quantized valley current flow on the boundary provided that inter-valley scattering can be neglected. This is in close analogy to the quantized edge spin current in QSHE [3, 4, 5]. Inter-valley scattering in graphene is well suppressed by the large momentum separation [31, 32, 33]. While these graphene

systems do not have nontrivial Z_2 topological order in the bulk [9, 10, 11, 12], the edge-states can nevertheless have the same features as those edge-states in QSHE, with the valley index playing the role of the spin. We further prove that these gapless edge-states are equivalent to the gapless chiral modes confined by topological domain wall in graphene, whose existence and chiral nature have been related to the valley-dependent bulk topological charge [34, 35]. Therefore, the peculiar edge-states on the boundary indeed share the same topological origin as the valley-dependent Hall effect in the bulk. This also opens up a new perspective to the existence of gapless chiral edge-states by contrasted topological charges in different regions of the Brillouin zone.

In the tight binding approximation with nearest neighbor hopping energy t , a single layer of graphene can be described by the following Hamiltonian

$$H = -t \sum_{\langle i,j \rangle} c_i^\dagger c_j + \sum_i U_i c_i^\dagger c_i, \quad (1)$$

where $\sum_{\langle i,j \rangle}$ sums over only nearest neighbor pairs. We consider a general situation where the bulk lattice can be subject to a staggered sublattice potential: $U_i = \Delta/2$ for sublattice \bullet , and $U_i = -\Delta/2$ for sublattice \circ (see Fig. 1(a)). On the boundary, graphene sheet terminated with the zigzag or the bearded edge preserves the two-valley band structure, and the edge-states form well known flat 1D bands which connect the two Dirac points [18, 19, 20]. We find that the edge-states are also gapped when the staggered sublattice potential is universally applied to all sites including those on the boundary. In Fig. 1(b) and (c), for clarity, only the edge-states on the left boundary are shown, while we note that an edge-state on the left boundary with wavevector k_y and energy E always has a counter part on the right boundary with k_y and $-E$. For the zigzag edge, the flat band appears in the region $k_y \in [\frac{2}{3}\pi, \frac{4}{3}\pi]$, while for bearded edge, it appears in the complementary region $k_y \notin [\frac{2}{3}\pi, \frac{4}{3}\pi]$. Here and hereafter, we normalize all length scale by the lattice constant a and all energy scale by the hopping energy t . Below, we focus on systems with zigzag edges, while qualitatively the same behaviors are always found in the systems with bearded edges.

Although the edge-states in the region $k_y \in [\frac{2}{3}\pi, \frac{4}{3}\pi]$ all have the same energy (Fig. 1(b)), their degree of localization in x direction varies. The edge-states near $k_y = \pi$ are almost completely localized on the outermost carbon atoms while those near the two Dirac points are much more spread into the bulk. Thereby, the energy response of the edge-states to potentials applied with unit cell length scale on the boundary will be different, which forms the basis for controlling the dispersion of the edge-band. The edge-bands on the two opposite boundaries can be individually controlled, and in Fig. 2 we demonstrate this controllability by tuning the on-site energy $U(L_1)$ on the outermost column L_1 (cf. Fig. 1(a)). Since the edge-state at $k_y = \pi$ is almost completely localized on column L_1 , its energy is just given by $U(L_1)$. Therefore, the edge-band dispersion bends upward when $U(L_1)$ increases [Fig. 2(a-d)]. When $U(L_1) = 1$, the edge-band completely

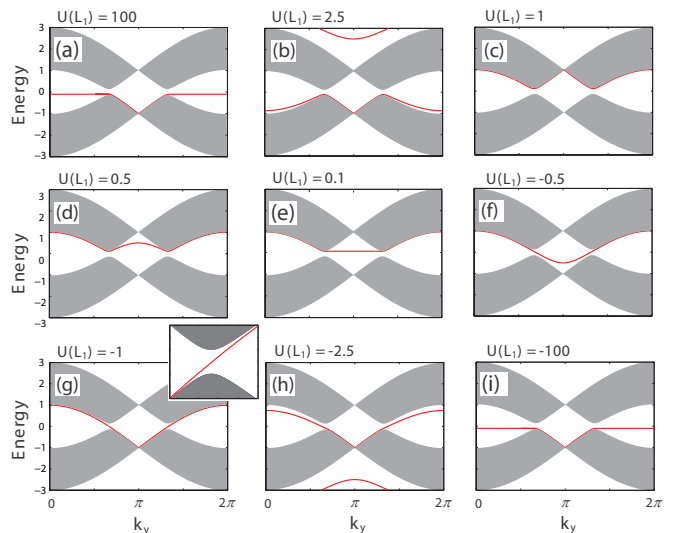


FIG. 2: (Color online) Band structure of single layer graphene with zigzag edges. A staggered sublattice potential $\Delta/2 = 0.1$ is applied throughout the sheet, while the on-site energies $U(L_1)$ of the outermost column L_1 (see Fig. 1(a)) are tuned to different values from positive to negative. (e) with $U(L_1) = \Delta/2 = 0.1$ is the same plot as Fig. 1(b). The inset in (g) is a blow up of the bulk gap region near $k_y = \frac{4}{3}\pi$. Only the edge-states on the left boundary are shown (red curves).

merges into the bulk conduction band continuum. With further increase of $U(L_1)$, the edge-band reappears on top of the bulk conduction continuum. Meantime, a new edge-band starts to peel off from the bulk valance continuum in the complementary region $k_y \notin [\frac{2}{3}\pi, \frac{4}{3}\pi]$ (Fig. 2(b)). This new edge-band will approach a flat dispersion at sufficiently large positive $U(L_1)$ (Fig. 2(a)), which is expected since carbon atoms in L_1 column is then effectively decoupled from neighboring columns and the graphene sheet effectively terminates with bearded edge (cf. Fig. 1(c)). The situation is similar when $U(L_1)$ is decreased to negative values [Fig. 2(f-i)]. The edge-band dispersion bends down initially and traverses the gap when $U(L_1) < -0.1$. At $U(L_1) = -1$, the edge-band merges into the bulk valance continuum. Most significantly, two gapless edge-modes with opposite velocity appear in the vicinity of the two Dirac points respectively (see Fig. 2(g) and inset).

The gapless edge-states usually reflect non-trivial topological orders in the bulk. In QHE, it is well known that the number of gapless chiral edge-states is given by the bulk Chern invariant [8]. This connection has been generalized to QSHE recently [9, 10, 11], where the existence of gapless chiral edge-states are dictated by a generalized definition of bulk Chern invariant [9], also known as the Z_2 topological invariant [10, 11]. To understand the edge-states in the present graphene system, we shall look into its bulk properties.

In the bulk, we can make a Fourier transform $c_{i,\bullet/\circ} \equiv \sum_{\mathbf{k}} c_{\mathbf{k},\bullet/\circ} e^{i\mathbf{k}\cdot\mathbf{R}_i}$ with \mathbf{R}_i being the lattice vector, and the

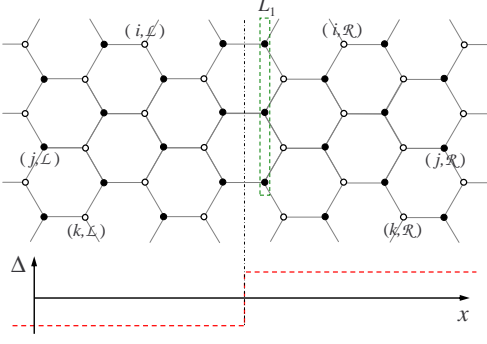


FIG. 3: (Color online) Schematic illustration of a topological domain wall. \bullet indicates carbon atoms with higher on-site energy $\frac{|\Delta|}{2}$, and \circ indicates carbon atoms with lower on-site energy $-\frac{|\Delta|}{2}$. The index of lattice sites i, j, k, \dots are arranged symmetrically about the domain wall in the regions to the left and to the right (denoted as \mathcal{L} and \mathcal{R} respectively).

Hamiltonian in Eq. (1) becomes

$$H_{\text{bulk}} = \sum_{\mathbf{k}} \begin{bmatrix} c_{\mathbf{k},\bullet}^\dagger & c_{\mathbf{k},\circ}^\dagger \end{bmatrix} \begin{bmatrix} \Delta/2 & V(\mathbf{k}) \\ V^*(\mathbf{k}) & -\Delta/2 \end{bmatrix} \begin{bmatrix} c_{\mathbf{k},\bullet} \\ c_{\mathbf{k},\circ} \end{bmatrix} \quad (2)$$

where $V(\mathbf{k}) = -(1 + e^{-i\mathbf{k}\cdot\mathbf{a}_1} + e^{-i\mathbf{k}\cdot\mathbf{a}_2})$, and $\mathbf{a}_{1,2}$ are the two primitive translation vectors (see Fig. 1(a)). Eq. (2) has the solutions of a conduction band $|u_{c,\mathbf{k}}\rangle$ and a valance band $|u_{v,\mathbf{k}}\rangle$. In order to describe the bulk topological property for the graphene system as an insulator, it is convenient to introduce a gauge potential and a gauge field in the valance band, defined as $\mathcal{A}(\mathbf{k}) \equiv \langle u_{v,\mathbf{k}} | i\nabla_{\mathbf{k}} | u_{v,\mathbf{k}} \rangle$ and $\Omega(\mathbf{k}) \equiv \nabla_{\mathbf{k}} \times \mathcal{A}$ respectively. This gauge field, known as the Berry curvature, is analogous to a magnetic field in the crystal momentum space. Its integral over a k -space area yields the Berry phase of an electron adiabatically going around the boundary of the area, which is similar to the relationship between a magnetic field and the Arharonov-Bohm phase. In 2D system, the Berry curvature vector is pointing out-of-plane and the Chern invariant is given by the flux of the Berry curvature threading the entire Brillouin zone $\mathcal{C} = \frac{1}{2\pi} \int_{BZ} d^2\mathbf{k} \Omega(\mathbf{k})$. For the graphene system described by Eq. (2), one finds the Berry curvature has a distribution sharply centered at the two Dirac points, $\Omega(\mathbf{q}) = \tau_z \frac{3\Delta}{2(\Delta^2 + 3q^2)^{3/2}}$, where $\tau_z = \pm$ is the index for the two valleys and \mathbf{q} is the wavevector measured from the Dirac points [16, 17]. We find the two valleys each carry a topological charge of $\tilde{N}_3 = \frac{1}{2\pi} \int d^2\mathbf{q} \Omega(\mathbf{q}) = \frac{1}{2} \tau_z \text{sgn}(\Delta)$, corresponding to a half-quantized valley Hall conductivity in the bulk [16, 17]. However, the Chern invariant is zero because of the time reversal symmetry in the system. It can be further shown that the Z_2 topological invariant also vanishes when the bulk gap is from inversion symmetry breaking only. Clearly, the gapless edge-states we found here do not have the same origin as those in the QHE and QSHE.

In searching for the topological origin of these edge-states, we notice that similar gapless valley-dependent chiral zero-modes also exist at topological domain walls in biased graphene bilayer, and the number and chiral nature of these

modes have been related to the valley-dependent topological charge \tilde{N}_3 in the bulk [34]. More specifically, in each valley, the topological charge ν of the zero-modes, i.e. the number of zero-modes moving in $+y$ direction minus the number of zero-modes moving in $-y$ direction, is equal to the difference of the bulk topological charges \tilde{N}_3 of the vacua on the two sides of the interface, $\nu = \tilde{N}_3(\text{right}) - \tilde{N}_3(\text{left})$ [34, 35]. For the single layer graphene under staggered sublattice potential, we can similarly consider a topological domain wall represented by a sharp kink in the order parameter Δ as shown in Fig. 3. Gapless chiral modes with topological charge $\nu = \tau_z$ is thus expected in the domain wall region [36]. Interestingly, $\nu = \tau_z$ is exactly the topological charge of the gapless edge-states shown in Fig. 2(g), when the on-site energy of the atoms on the outermost column is equal to the nearest neighbor hopping energy. Below, we show the intrinsic connection between the gapless zero-modes in the domain wall and the gapless edge-states on the boundary.

Graphene with the above mentioned topological domain wall can be described by the following Hamiltonian

$$H = - \sum_{\langle i,j \rangle} c_{i,S}^\dagger c_{j,S} + \sum_i U_{i,S} c_{i,S}^\dagger c_{i,S} \quad (3)$$

$$- \sum_{\langle i,j \rangle} c_{i,A}^\dagger c_{j,A} + \sum_i U_{i,A} c_{i,A}^\dagger c_{i,A}$$

where the index i, j here run over lattice sites on one side of the domain wall. $c_{j,A} \equiv \frac{1}{\sqrt{2}}(c_{j,\mathcal{R}} - c_{j,\mathcal{L}})$ and $c_{j,S} \equiv \frac{1}{\sqrt{2}}(c_{j,\mathcal{R}} + c_{j,\mathcal{L}})$ describe respectively the antisymmetric and symmetric combination of wavefunction on the two sites (i, \mathcal{L}) and (i, \mathcal{R}) located symmetrically on the two sides of the domain wall (see Fig. 3). For i in the nearest column to the domain wall (L_1 in Fig. 3), we have $U_{i,S} = -1 + \frac{|\Delta|}{2}$ and $U_{i,A} = 1 + \frac{|\Delta|}{2}$ respectively, while for all other lattice sites, both $U_{i,A}$ and $U_{i,S}$ are equal to $\frac{|\Delta|}{2}$ on sublattice \bullet and equal to $-\frac{|\Delta|}{2}$ on sublattice \circ . In this way, we establish the equivalence between an extended graphene with a domain wall and a semi-infinite graphene with one zigzag edge subjected to certain boundary potential. In particular, the gapless chiral zero-modes in the domain wall are of symmetric wavefunction and are equivalent to the gapless edge-states on the boundary when on-site energy of the outermost column is $-1 + \frac{|\Delta|}{2}$ (cf. Fig. 2(g)). Therefore, the number of gapless edge-states in the latter situation is also determined by the bulk topological charge \tilde{N}_3 in the two valleys.

We note that the edge-states can evolve continuously from the gapless chiral modes near the Dirac points to the flat dispersion band connecting the two Dirac points by tuning the magnitude of the boundary potential only, during which the bulk property is unchanged. Therefore, these edge-states spectra shall all have the same origin from the valley-dependent bulk topological charge, and in particular, the number of edge-band is determined by the value of \tilde{N}_3 .

Finally, we turn our attention to a different graphene system, the bilayer graphene with Bernal stacking. By applying

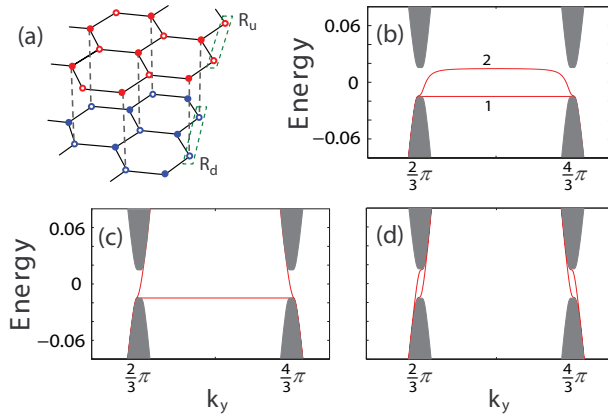


FIG. 4: (Color online) (a) Schematic illustration of a graphene bilayer. (b) Band structure of a biased graphene bilayer with zigzag edges. The on-site energy is universally -0.015 in the upper layer and 0.015 in the lower layer. We assume the nearest neighbor intralayer hopping energy $t = 1$ and interlay hopping energy $t_{\perp} = 0.14$ respectively. Only the edge-states on the right boundary are shown (red curves). (c) Band structure when the on-site energies of the outermost column R_d in the lower layer are tuned to $U(R_d) = 1$. (d) Band structure when the on-site energies of the outermost columns in both layers are $U(R_d) = U(R_u) = 1$.

a bias Δ between the two layers, a bulk gap can be induced and it has been shown that, in the insulating states, the two valleys carry the topological charge of $\tau_z \text{sgn}(\Delta)$ in the highest valance band [16, 17, 34]. By the above topological argument, similar edge-states behaviors to those in the single layer shall be expected. In Fig. 4, we show the edge-states spectrum when the on-site energy is universally -0.015 in the top layer and 0.015 in the bottom layer. As expected, each boundary now carry two bands [23]. Edge band 1 has a flat dispersion in the region $k_y \in [\frac{2}{3}\pi, \frac{4}{3}\pi]$, similar to the edge-band in the single layer case, and we find that the states near $k_y = \pi$ are completely localized on the outermost column (R_u) of the upper layer. Edge band 2 also has a flat dispersion near $k_y = \pi$, but acquires finite valley-dependent velocity near the Dirac points [23]. The two edge-bands have an energy difference equal to $\Delta = -0.03$ in the flat region, which is due to the fact that, in edge-band 2, the states near $k_y = \pi$ are localized on the outermost column (R_d) in the lower layer. Thereby, the dispersion of the two edge-bands can be individually controlled by tuning on-site energies of R_u and R_d columns respectively. In particular, depending on the boundary potential, we can have either one or two valley-dependent gapless chiral modes per valley per boundary, as shown in Fig. 4(c) and (d). In fact, the gapless edge-states when $U(R_u) = U(R_d) = 1$ are equivalent to the symmetric modes confined by a line dislocation so that the bilayer is of AB stacking to the left of this topological line defect and is of BA stacking to the right of the defect [37]. The topological charge of these gapless modes $\nu = -2\tau_z$ in each valley, which is found consistent with the bulk topological charge $\tilde{N}_3 = -\tau_z$. Indeed, in bilayer graphene, the behaviors of the edge-states are also de-

termined by the valley-dependent topological charges in the bulk.

The work was supported by NSF, DOE, the Welch Foundation, and NSFC.

-
- [1] R. B. Laughlin, Phys. Rev. B **23**, 5632 (1981).
 - [2] B. I. Halperin, Phys. Rev. B **25**, 2185 (1982).
 - [3] C. L. Kane and E. J. Mele, Phys. Rev. Lett. **95**, 226801 (2005).
 - [4] C. Wu, B. A. Bernevig, and S.-C. Zhang, Phys. Rev. Lett. **96**, 106401 (2006).
 - [5] B. A. Bernevig, T. L. Hughes, and S.-C. Zhang, Science **314**, 1757 (2006).
 - [6] M. Onoda and N. Nagaosa, Phys. Rev. Lett. **95**, 106601 (2005).
 - [7] D. J. Thouless, M. Kohmoto, M. P. Nightingale, and M. den Nijs, Phys. Rev. Lett. **49**, 405 (1982).
 - [8] Y. Hatsugai, Phys. Rev. Lett. **71**, 3697 (1993).
 - [9] X.-L. Qi, Y.-S. Wu, and S.-C. Zhang, Phys. Rev. B **74**, 045125 (2006).
 - [10] C. L. Kane and E. J. Mele, Phys. Rev. Lett. **95**, 146802 (2005).
 - [11] L. Fu and C. L. Kane, Phys. Rev. B **74**, 195312 (2006).
 - [12] J. E. Moore and L. Balents, Phys. Rev. B **75**, 121306 (2007).
 - [13] K. S. Novoselov, A. K. Geim, S. V. Morozov, D. Jiang, M. I. Katsnelson, I. V. Grigorieva, S. V. Dubonos, and A. A. Firsov, Nature **438**, 197 (2005).
 - [14] Y. Zhang, Y.-W. Tan, H. L. Stormer, and P. Kim, Nature **438**, 201 (2005).
 - [15] A. K. Geim and K. S. Novoselov, Nature Mater. **6**, 183 (2007).
 - [16] D. Xiao, W. Yao, and Q. Niu, Phys. Rev. Lett. **99**, 236809 (2007).
 - [17] W. Yao, D. Xiao, and Q. Niu, Phys. Rev. B **77**, 235406 (2008).
 - [18] K. Nakada, M. Fujita, G. Dresselhaus, and M. S. Dresselhaus, Phys. Rev. B **54**, 17954 (1996).
 - [19] S. Ryu and Y. Hatsugai, Phys. Rev. Lett. **89**, 077002 (2002).
 - [20] L. Brey and H. A. Fertig, Phys. Rev. B **73**, 235411 (2006).
 - [21] N. M. R. Peres, A. H. Castro Neto and F. Guinea, Phys. Rev. B **73**, 195411 (2006).
 - [22] N. M. R. Peres, F. Guinea and A. H. Castro Neto, Phys. Rev. B **73**, 125411 (2006).
 - [23] E. V. Castro, N. M. R. Peres, J. M. B. Lopes dos Santos, A. H. Castro Neto and F. Guinea, Phys. Rev. Lett. **100**, 026802 (2008).
 - [24] A. H. Castro Neto, F. Guinea, N. M. R. Peres, K. S. Novoselov, and A. K. Geim, arXiv:0709.1163, (2008).
 - [25] A. Rycerz, J. Tworzydło, and C. W. J. Beenakker, Nature Phys. **3**, 172 (2007).
 - [26] B. Wunsch, T. Stauber, F. Sols, and F. Guinea, Phys. Rev. Lett. **101**, 036803 (2008).
 - [27] K. Sawada, F. Ishii, and M. Saito, Appl. Phys. Express **1**, 064004 (2008).
 - [28] O. V. Yazyev and M. I. Katsnelson, Phys. Rev. Lett. **100**, 047209 (2008).
 - [29] S. Bhowmick and V. B. Shenoy, J. Chem. Phys. **128**, 244717 (2008).
 - [30] K. Sasaki, J. Jiang, R. Saito, S. Onari, and Y. Tanaka, J. Phys. Soc. Jpn. **76**, 033702 (2007).
 - [31] S. V. Morozov, K. S. Novoselov, M. I. Katsnelson, F. Schedin, L. A. Ponomarenko, D. Jiang, and A. K. Geim, Phys. Rev. Lett. **97**, 016801 (2006).
 - [32] A. F. Morpurgo and F. Guinea, Phys. Rev. Lett. **97**, 196804 (2006).

- [33] R. V. Gorbachev, F. V. Tikhonenko, A. S. Mayorov, D. W. Horsell, and A. K. Savchenko, Phys. Rev. Lett. **98**, 176805 (2007).
- [34] I. Martin, Y. M. Blanter, and A. F. Morpurgo, Phys. Rev. Lett. **100**, 036804 (2008).
- [35] G. E. Volovik, *The Universe in a Helium Droplet* (Oxford University Press, 2003).
- [36] G. W. Semenoff V. Semenoff, and Fei Zhou Phys. Rev. Lett. **101**, 087204 (2008).
- [37] Note that this is a different type of topological domain wall from the one explored in Ref. [34].